

RADIATION FROM SLITS ON FERRITE-FILLED PARALLEL PLATES WITH A SUPERSTRATE

Keum C. Hwang and Hyo J. Eom
Department of Electrical Engineering and Computer Science
Korea Advanced Institute of Science and Technology
373-1, Guseong-dong, Yuseong-gu, Daejeon, Korea
E-mail: hjeom@ee.kaist.ac.kr

1. INTRODUCTION

A dielectric superstrate has been widely used to improve the low efficiency and low gain of antennas. For instance, research works for microstrip antennas covered by a superstrate have been reported [1-3]. The experiments for a single microstrip patch antenna with a dielectric superstrate have been performed [4]. The resonance condition for high gain enhancement can be achieved by adjusting the distance between a radiating element and superstrate. Extremely high gain enhancement using multilayered superstrates has been reported in [5]. The purpose of the present paper is to investigate the effect of a superstrate on the radiation performance of aperture array antenna. This paper presents an analysis of radiation from multiple slits on a ferrite-filled parallel plates with a superstrate. Our analysis is based on the Fourier transform and mode matching [6], which yields a fast convergent series solution. To demonstrate the validity of our theoretical approach, the computational results are compared with the simulation data of Microwave Studio of CST.

2. FIELD ANALYSIS

Figure 1 shows a leaky wave antenna consisting of a ferrite-filled parallel plates with a superstrate. Similar leaky wave antennas without a superstrate have been investigated in [6, 7] using the Fourier transform and mode matching. No field variation is assumed in the y -direction, thereby making the antenna geometry two-dimensional. The $\exp(-i\omega t)$ time convention is suppressed throughout the analysis. Assume that an incident TE_s mode propagates along the x -direction in the ferrite-filled parallel plates. For theoretical convenience, some of the field representations in [7] are used here. The permittivity and tensor permeability of ferrite-loaded medium are ϵ_f and $\bar{\mu}$, respectively. The direction of the applied DC magnetic field is parallel to the y -axis and the permeability tensor is given by

$$\bar{\mu} = \mu_0 \begin{bmatrix} \mu & 0 & iK \\ 0 & 1 & 0 \\ -iK & 0 & \mu \end{bmatrix} \quad (1)$$

where $\mu = 1 + \frac{\omega_m(\omega_o - i\alpha\omega)}{(\omega_o - i\alpha\omega)^2 - \omega^2}$, $K = \frac{\omega_m\omega}{(\omega_o - i\alpha\omega)^2 - \omega^2}$, $\omega_o = \gamma H_{in}$, $\omega_m = \gamma 4\pi M_s$, α is the damping factor, γ is the gyromagnetic ratio of ferrite, H_{in} is the internal DC magnetic field within ferrite, and $4\pi M_s$ is the saturation magnetization of ferrite. The effect of ferrite linewidth is included in terms of α .

The incident and scattered electric fields in region (I) ($-b < z < 0$) are

$$E_{yi}^I(x, z) = \sin k_{zs}(z+b)e^{ik_{xs}(x+x_i)} \quad (2)$$

$$E_{ys}^I(x, z) = \frac{i}{\pi} \int_{-\infty}^{\infty} \tilde{E}_y^I(\zeta) \sin(\kappa_1 z) e^{-i\zeta x} d\zeta \quad (3)$$

where $k_{zs} = \frac{s\pi}{b}$, $k_{xs} = \sqrt{k_1^2 - k_{zs}^2}$, $\kappa_1 = \sqrt{k_1^2 - \zeta^2}$, $\mu_f = \frac{\mu^2 - K^2}{\mu}$, and $k_1 = \omega\sqrt{\mu_0\mu_f\varepsilon_0\varepsilon_f}$.

Note that the x_i is the half length of a ferrite slab. In region (II) ($-b-d < z < -b$), the scattered electric field is

$$E_{ys}^{II}(x, z) = \sum_{m=1}^{\infty} \sin a_m (x + a - lT) \left[b_m^l \cos \xi_m (z + b) + c_m^l \sin \xi_m (z + b) \right] \quad (4)$$

where $a_m = \frac{m\pi}{2a}$, $\xi_m = \sqrt{k_2^2 - a_m^2}$, and $k_2 = \omega\sqrt{\mu_0\mu_2\varepsilon_0\varepsilon_2}$. In regions (III), (IV) and (V), the scattered electric fields are represented as, respectively,

$$E_{ys}^{III}(x, z) = \frac{1}{2\pi} \int_{-\infty}^{\infty} \left[\tilde{E}_{III}^+(\zeta) e^{i\kappa_3(z+h_1)} + \tilde{E}_{III}^-(\zeta) e^{-i\kappa_3(z+h_1)} \right] e^{-i\zeta x} d\zeta \quad (5)$$

$$E_{ys}^{IV}(x, z) = \frac{1}{2\pi} \int_{-\infty}^{\infty} \left[\tilde{E}_{IV}^+(\zeta) e^{i\kappa_4(z+h_2)} + \tilde{E}_{IV}^-(\zeta) e^{-i\kappa_4(z+h_2)} \right] e^{-i\zeta x} d\zeta \quad (6)$$

$$E_{ys}^V(x, z) = \frac{1}{2\pi} \int_{-\infty}^{\infty} \tilde{E}_y^V(\zeta) e^{-i\kappa_5(z+h_2)} e^{-i\zeta x} d\zeta \quad (7)$$

where $\kappa_q = \sqrt{k_q^2 - \zeta^2}$, $k_q = \omega\sqrt{\mu_0\mu_q\varepsilon_0\varepsilon_q}$, and $q = 3, 4, 5$.

To determine the unknown modal coefficients b_m^l and c_m^l , the boundary conditions of E_y and H_x continuities must be enforced at each boundary. Enforcing the boundary conditions in conjunction with the mode matching and Fourier transform [6, 7] results in a set of simultaneous equations for the discrete modal coefficients b_m^l and c_m^l . The radiated far-zone power density in region (V) is given in terms of b_m^l and c_m^l as

$$p_s(r, \theta_s) = \frac{k_5}{4\pi r \eta_0} \cos^2 \theta_s |K(\theta_s)|^2 \quad (8)$$

where

$$K(\theta_s) = \sum_{l=-L_4}^{L_2} \sum_{m=1}^{\infty} a_m \left[b_m^l \cos \xi_m d - c_m^l \sin \xi_m d \right] e^{ik_5 \sin \theta_s lT} \cdot \frac{\kappa_4 F_m(\zeta)}{\kappa_4 \cos(\kappa_4 c) - i\kappa_5 \sin(\kappa_4 c)} \frac{A(\zeta) + B(\zeta)}{A(\zeta) e^{i\kappa_3 h} + B(\zeta) e^{-i\kappa_3 h}} \Bigg|_{\zeta = k_5 \sin \theta_s}, \quad (9)$$

$$A(\zeta) = \kappa_4 (\kappa_3 - \kappa_5) - i\kappa_3 \kappa_5 \tan(\kappa_4 c) + i\kappa_4^2 \tan(\kappa_4 c), \quad (10)$$

$$B(\zeta) = \kappa_4 (\kappa_3 + \kappa_5) - i\kappa_3 \kappa_5 \tan(\kappa_4 c) - i\kappa_4^2 \tan(\kappa_4 c), \quad (11)$$

and

$$F_m(v) = \frac{e^{iva}(-1)^m - e^{-iva}}{v^2 - a_m^2}. \quad (12)$$

Equation (8) represents a fast convergent series for radiation from a ferrite-filled leaky wave antenna with a superstrate.

3. NUMERICAL RESULTS

Figure 2 illustrates the radiation efficiency for N (the number of slots)=1 when $a=4.95$ mm, $b=6.7$ mm, $c=2.54$ mm, $d=2.1$ mm, $x_i=70$ mm, $4\pi M_s=1300$ G, $\Delta H=0$ oe, $H_{in}=0$ oe, $\epsilon_f=11.8$, $\epsilon_4=10.8$, and $\epsilon_2=\epsilon_3=\epsilon_5=1$. Without a superstrate, the radiation efficiency increases monotonously from 8.5 GHz to 11.5 GHz. When the distance between slots and a superstrate h is 16.5 mm and 14.5 mm, the other peaks are observed at 9 GHz and 10 GHz, respectively, due to the presence of a superstrate. Note that the distance h satisfies the resonance condition ($h=0.5\lambda_0$) to achieve gain enhancement [3, 4].

Figures 3 and 4 show the normalized H-plane radiation patterns for multiple slots ($N=9$). The operating frequency is 10.05 GHz, slot period $T=11.7$ mm, and the rest of antenna dimensions are the same as those in Fig. 1. The ferrite used in our computation is commercially available one (TT1-109, Trans-Tech). As H_{in} increases from 0 to 1033 oe, the radiated main beam scans about 17° ($-11^\circ \sim 6^\circ$). To demonstrate the validity of our theoretical approach, our radiation patterns are compared with the simulation data of Microwave Studio of CST. Figures 3 and 4 show a favorable agreement between our results and the simulation data.

Figure 5 shows the main beam intensity versus the distance h at 10.05 GHz. The antenna dimensions and the applied DC magnetic field are the same as those in Fig. 3. The main beam intensity of the antenna without a superstrate is shown as a reference. When the distance $h=13$ mm, the maximum of main beam intensity is observed, where the intensity is 4.5 dB higher than that without a superstrate.

4. CONCLUSION

Radiation from multiple slits on ferrite-filled parallel plates with a superstrate is investigated using the Fourier transform and mode matching techniques. Our computational results favorably compare with other simulation data. Use of a superstrate layer has an advantages of gain enhancement when the distance between slots and a superstrate satisfies the resonance condition.

REFERENCES

- [1] D. R. Jackson and N. G. Alexopoulos, "Gain enhancement methods for printed circuit antennas," *IEEE Trans. Antennas Propagat.*, vol. 33, no. 9, pp. 976-987, Sept. 1985.
- [2] G. V. Eleftheriades and M. Simcoe, "Gain and efficiency of linear slot arrays on thick substrates for millimeter-wave wireless applications," *IEEE Int. Symp. Antennas Propagat.*, vol. 4, pp. 2428-2431, July 1999.
- [3] W. Choi, C. Pyo, Y. H. Cho, J. Choi, and J. Chae, "High gain and broadband microstrip patch antenna using a superstrate layer," *IEEE Int. Symp. Antennas Propagat.*, vol. 2, pp. 292-295, June 2003.
- [4] X. H. Shen, P. Delmotte, and G. A. E. Vandenbosch, "Effect of superstrate on radiated field of probe fed microstrip patch antenna," *IEE Proc. Microw. Antennas Propagat.*, vol. 148, no. 3, pp. 141-146, June 2001.
- [5] H. Y. Yang and N. G. Alexopoulos, "Gain enhancement methods for printed circuit antennas through multiple superstrates," *IEEE Trans. Antennas Propagat.*, vol. 35, no. 7, pp. 860-863, July 1987.
- [6] J. H. Lee, H. J. Eom, and J. W. Lee, "Scattering and radiation from finite thick slits in parallel-plate waveguide," *IEEE Trans. Antennas Propagat.*, vol. 40, no. 2, pp. 212-216, Feb. 1996.
- [7] K. C. Hwang and H. J. Eom, "Radiation from a ferrite-filled rectangular waveguide with multiple slits," *IEEE Microwave Wireless Compon. Lett.*, accepted for publication, 2004.

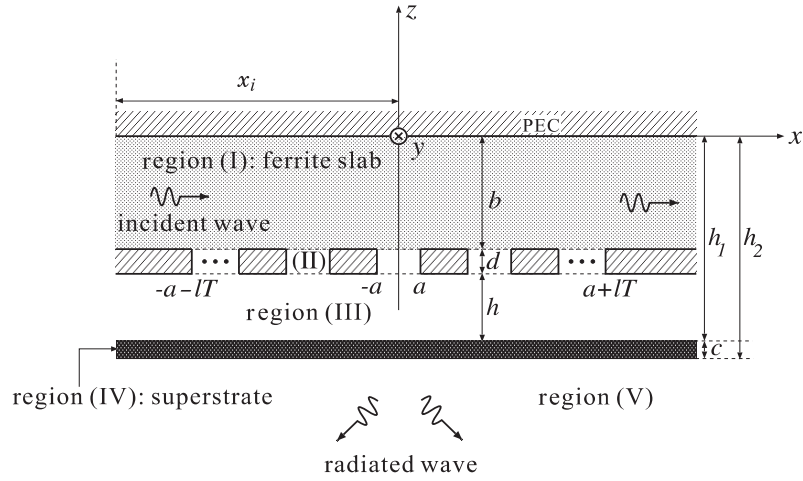


Figure 1. Problem geometry

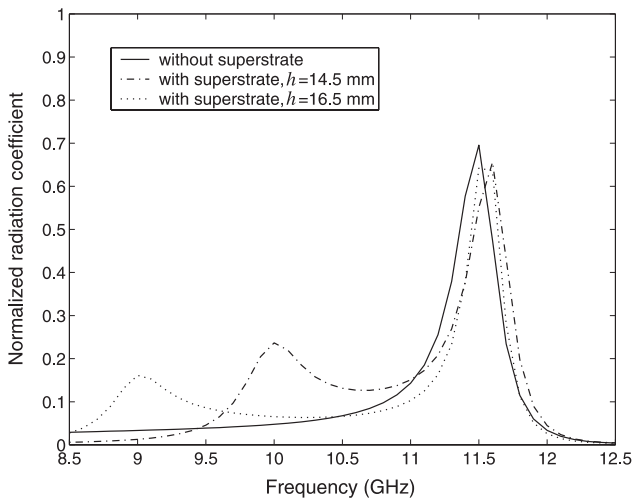


Figure 2. Radiation efficiency

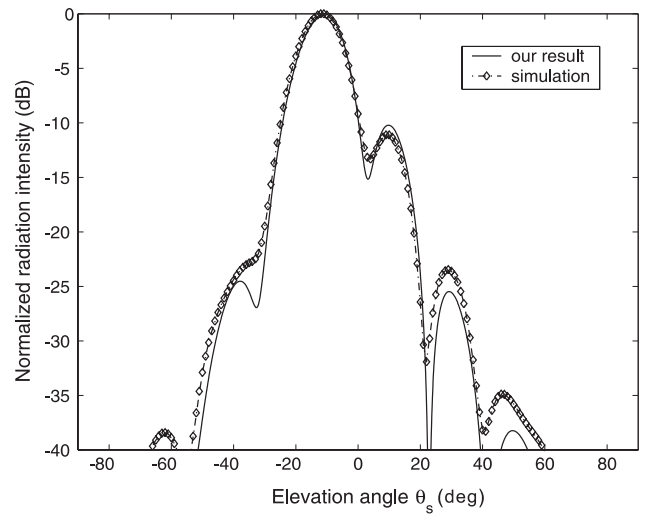


Figure 3. Normalized H-plane radiation pattern, $h = 13.0$ mm, $H_{in} = 0$ oe

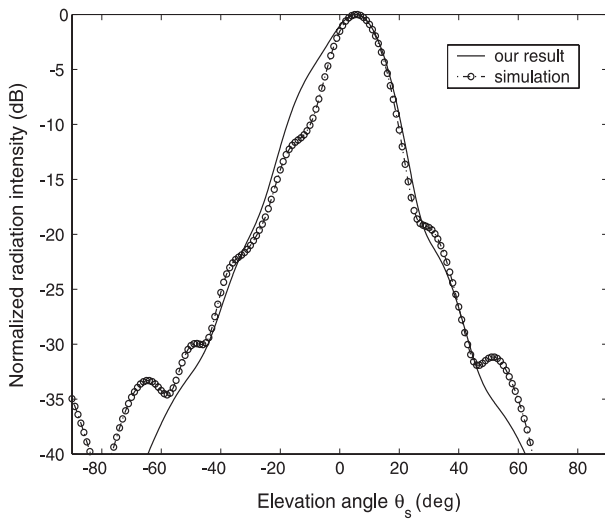


Figure 4. Normalized H-plane radiation pattern, $h = 13.0$ mm, $H_{in} = 1033$ oe

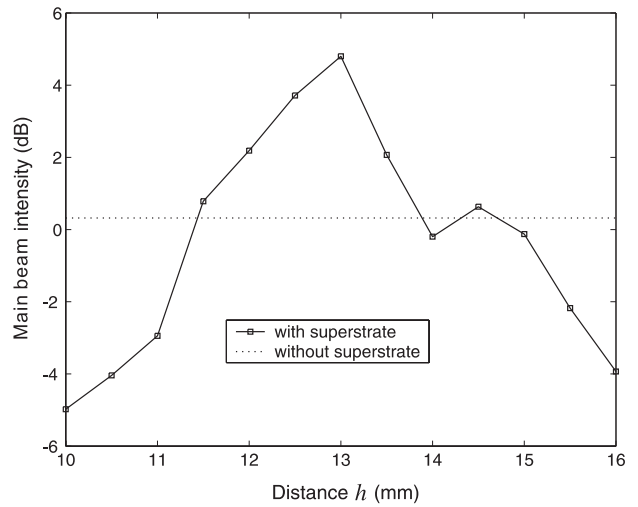


Figure 4. Maximum radiation intensity versus the distance h